FEBS Letters 586 (2012) 545–556

FEBS Letters

journal homepage: www.FEBSLetters.org

Review

NAD(H)-coupled hydrogen cycling – structure–function relationships of bidirectional [NiFe] hydrogenases

M. Horch [a], L. Lauterbach [b], O. Lenz [b], P. Hildebrandt [a], I. Zebger [a,*]

[a] Technische Universität Berlin, Institut für Chemie, Sekr. PC 14, Straße des 17. Juni 135, D-10623 Berlin, Germany
[b] Humboldt-Universität zu Berlin, Institut für Biologie/Mikrobiologie, Chausseestraße 117, 10115 Berlin, Germany

ARTICLE INFO

Article history:
Received 31 August 2011
Revised 5 October 2011
Accepted 6 October 2011
Available online 2 November 2011

Edited by Miguel Teixeira and Ricardo O. Louro

Keywords:
Biocatalysis
Hydrogenase
Spectroscopy
Oxygen tolerance
NADH regeneration
Biofuel

ABSTRACT

Hydrogenases catalyze the activation or production of molecular hydrogen. Due to their potential importance for future biotechnological applications, these enzymes have been in the focus of intense research for the past decades. Bidirectional [NiFe] hydrogenases are of particular interest as they couple the reversible cleavage of hydrogen to the redox conversion of NAD(H). In this account, we review the current state of knowledge about mechanistic aspects and structural determinants of these complex multi-cofactor enzymes. Special emphasis is laid on the oxygen-tolerant NAD(H)-linked bidirectional [NiFe] hydrogenase from *Ralstonia eutropha*.

1. Introduction

In all living systems, energy conversion involves the oxidation of primary electron donors. In this context, hydrogenases [1], as versatile ancient metalloproteins, enable the microbial cell to utilize dihydrogen as an energy source by catalyzing its reversible cleavage into protons and electrons: $H_2 \leftrightarrow 2H^+ + 2e^-$. Via this reaction, these enzymes can also provide reducing equivalents for biosynthesis and contribute to the disposal of excess electrons by hydrogen evolution [2]. Furthermore, regulatory hydrogenases are able to adjust these processes to the respective environmental conditions via transcriptional regulation of genes encoding for energy-transforming hydrogenases [3,4].

Due to their potential applicability in biotechnological processes, hydrogenases have been extensively studied. Envisaged applications are mainly related to bio-energetic approaches, i.e., energy conversion in enzymatic fuel cells or biohydrogen production [5]. In addition, hydrogenases are promising model systems to investigate electron transfer processes in complex multi-cofactor enzymes and might also serve as "blueprints" for hydrogen activating, biomimetic compounds.

For several decades, spectroscopic studies have contributed essentially to the understanding of hydrogenases by providing insights into cofactor composition, electronic, structural, and redox properties of these enzymes. In the following, we will give an overview on the present state of research on bidirectional [NiFe] hydrogenases that couple reversible hydrogen conversion to the evolution and consumption of NADH. Here, emphasis will be placed on spectroscopic studies to elucidate structure–function relationships. Previous and recent insights are reviewed and discussed in conjunction with open questions and challenges for future research.

2. [NiFe] Hydrogenases: an overview

With regard to the metal content of the active site, hydrogenases can be classified into three phylogenetically unrelated groups [2]: [FeFe] hydrogenases with two Fe atoms at the catalytic center [6], [Fe] hydrogenases that harbor an Fe-guanylylpyridinol cofactor [7], and [NiFe] hydrogenases, where hydrogen conversion takes place at a heterobimetallic active site containing Ni and Fe [8,9]. Apart from [Fe] hydrogenases, all of these enzymes comprise additional Fe–S clusters for electron transfer to or from the active site.

2.1. General structural properties

[NiFe] hydrogenases are composed of at least two different subunits (Fig. 1A and B): a large one, which contains the deeply buried

* Corresponding author.
E-mail address: ingo.zebger@tu-berlin.de (I. Zebger).

0014-5793 © 2011 Federation of European Biochemical Societies. Published by Elsevier B.V. Open access under CC BY-NC-ND license.
doi:10.1016/j.febslet.2011.10.010

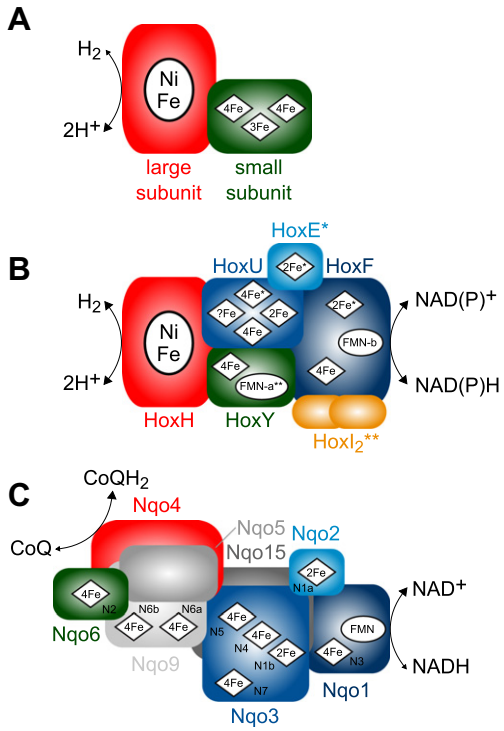

Fig. 1. Schematic representation of (A) "standard" [NiFe] hydrogenases, (B) NAD(H)-linked bidirectional [NiFe] hydrogenases, and (C) the peripheral part of the respiratory Complex I [8,10,57,69,124]. Homologous subunits are represented with the same color with HoxF exhibiting sequence homology to both Nqo1 and Nqo2 of Complex I. Subunit interactions of HoxE are tentatively depicted based on comparison with the homologous Nqo2 subunit of the respiratory Complex I. "2Fe" and "4Fe" refer to [2Fe–2S] and [4Fe–4S] clusters, respectively. "?Fe" is most likely a [4Fe–4S] cluster, although a [3Fe–4S] cluster in certain bidirectional hydrogenases cannot be entirely excluded (see text). *Not observed in aerobic bidirectional hydrogenases from *R. eutropha* and *R. opacus*. HoxE and the included [2Fe–2S] cluster appear to be absent from the Hox2 bidirectional hydrogenase from *Thiocapsa roseopersicina*, too. [125] **Only reported for the bidirectional hydrogenase from *R. eutropha*. [60].

active site, and a small one, harboring at least one [4Fe–4S] cluster close to the active site (proximal cluster). The large and small subunit exhibit sequence homology to the Nqo4 and Nqo6 subunit[1] of NADH:ubiquinone oxidoreductase (Complex I), respectively (Fig. 1C) [10,11]. In oxygen sensitive "standard" [NiFe] hydrogenases, which are located at the periplasmic face of the cytoplasmic membrane, the electron relay in the small subunit is extended by a distal [4Fe–4S] cluster, and a medial [3Fe–4S] cluster between the two cubanes (Figs. 1A and 2) [8]. In addition to the two metal centers, the active site of these enzymes contains four conserved cysteinyl thiolate donors, two of which serve as bridging ligands between Ni and Fe, while the other two are solely bound to Ni (Fig. 2). In addition, the Fe is coordinated by three non-proteinaceous ligands, i.e., two cyanides and one CO molecule, all of which are unprecedented in biological systems other than hydrogenases [9,12,13]. While the Ni is redox active during activation and catalysis, the Fe remains in the Fe(II) low-spin configuration due to these strong-field inorganic ligands. It is generally accepted that hydrogen cycling involves an additional ligation site bridging the two metals [14]. Hydrophobic cavities for hydrogen diffusion between the active site and the protein surface as well as putative proton transfer pathways have been also described for "standard" [NiFe] hydrogenases [15,16].

[1] The subunit nomenclature of Complex I from *Thermus thermophilus* [10] will be used throughout the paper.

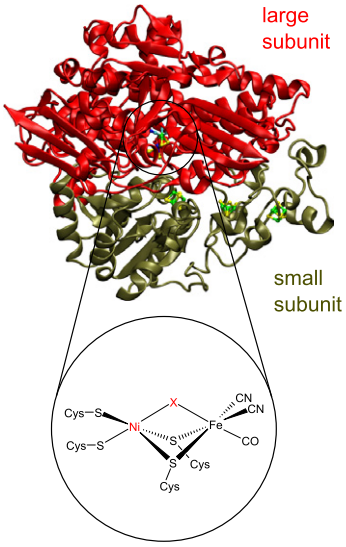

Fig. 2. Crystal structure of the "standard" [NiFe] hydrogenase from *D. gigas* [8] with the large and small subunit depicted in red and green, respectively. The [NiFe] active site is enlarged for a better visualization. Its redox state is primarily determined by the oxidation state of the Ni ion, and the exchangeable ligand "X" at the third bridging site between Ni and Fe (both highlighted in red).

2.2. Redox states of the [NiFe] center and the catalytic cycle

Applying infrared (IR) spectroscopy, various active and inactive redox states of the catalytic center from "standard" [NiFe] hydrogenases have been identified by the characteristic stretching vibrations of the three inorganic ligands (Fig. 3) [17,18]. All of these species primarily differ with respect to the redox state of the Ni and the chemical nature of the exchangeable ligand "X" in the bridging position between the two metals (Figs. 2 and 3). Electron paramagnetic resonance (EPR) spectroscopy, on the other hand, selectively monitors paramagnetic species of all cofactors. In the inactive oxidized state, two species with different activation kinetics have been identified, both revealing EPR signals characteristic for Ni(III): The so-called "ready" Ni_r-B state that is proven to carry a hydroxo ligand in the bridging position between the two metals [19,20] can easily be (re-)activated in the presence of hydrogen. In contrast, reductive activation of the "unready" Ni_u-A species takes hours [21]. This property has been tentatively related to the presence of a (hydro)peroxo species in the bridging position or thiolato oxygenation at the active site cysteines [20,22]. One-electron reduction of Ni_u-A and Ni_r-B yields the corresponding EPR-silent Ni(II) species Ni_u-S and Ni_r-S, respectively. Both forms are also catalytically inactive, as they supposedly still carry the respective oxygen species of Ni_u-A and Ni_r-B. Two sub-species of the Ni_r-S state have been identified and suggested to differ with respect to the protonation state [17,23–25]. A loosely bound water molecule might be rapidly released from the protonated sub-form, resulting in the catalytically active Ni_a-S state with a vacant coordination site between the two metals. Further one-electron reduction of this state yields the paramagnetic Ni(III) species Ni_a-C, which is considered to be the central intermediate of hydrogen cycling in "standard" [NiFe] hydrogenases. This view is based on experimental and theoretical studies, revealing a hydride as the additional bridging ligand in this species [18,26]. The fully reduced Ni_a-SR state, which is formed by one-electron reduction of Ni_a-C, presumably also contains a hydride in the bridging position [25,27]. This EPR-silent Ni(II) species, commonly assigned to another step of the catalytic cycle, reveals up to three sub-forms, which might differ with respect to the conformation, protonation or spin state of the

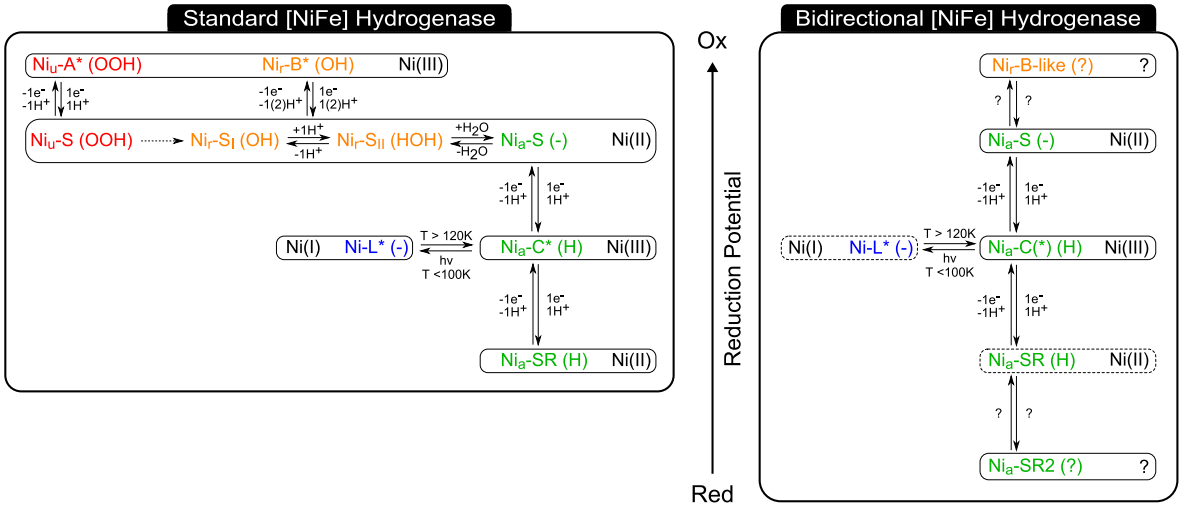

Fig. 3. Essential redox states and interconversions of the active site of "standard" [NiFe] hydrogenases and NAD(H)-linked bidirectional [NiFe] hydrogenases from *R. eutropha* H16 and *Synechocystis* sp. PCC6803.[24,25,88,89] "Unready" and "ready" inactive states are shown in red and orange, respectively, while catalytically active species are depicted in green. Ni–L is represented in blue as the involvement of this species in the catalytic cycle is under debate [18,24]. The (proposed) chemical nature of the bridging ligand at the active site is indicated in parentheses for each individual redox species. EPR detected states are marked with an asterisk. For bidirectional hydrogenases, dashed boxes indicate redox states that have been detected in *R. eutropha*, but so far not in *Synechocystis* sp. For the enzyme from the latter organism, an intermediate species has been observed by IR spectroscopy, which could be tentatively assigned to the Ni_a-C state. So far, this redox state could not be enriched for EPR studies. Therefore, its identity still has to be proven [89]. For the sake of clarity, redox states of the enzyme from *R. eutropha* that were detected under non-native conditions [90] are not included in the present scheme.

[NiFe] complex [27,28]. Alternatively, these sub-species have been suggested to harbor different Ni-bound and/or bridging ligands, such as H^- and/or H_2 [29]. At cryogenic temperatures, irradiation of the Ni_a-C state with white light induces a further EPR-detectable species (Ni-L) [30], which is formed via photo-dissociation of the bridging hydride [26]. Although this state is created under non-physiological conditions, a similar, transient Ni(I) species is widely claimed to be involved in hydrogen cycling [31–33].

Different models have been suggested for the catalytic cycle of [NiFe] hydrogenases. Most of them propose a heterolytic cleavage of hydrogen, where the hydride is reversibly bound between the two metals while one of the terminal cysteinyl thiolates acts as a proton acceptor [32]. However, there is still no consensus about the detailed mechanism as well as the type and number of intermediate states involved. An alternative catalytic cycle proposed recently suggests an initial heterolytic cleavage of hydrogen followed by an oxidative addition mechanism during turnover [31]. Irrespective of the exact reaction mechanism, the reversible formation of a H_2 σ-bond complex has been suggested as an essential initial event for hydrogen activation at transition metal sites [34].

3. Bidirectional hydrogenases: versatile players in biological hydrogen conversion

[NiFe] hydrogenases can be further divided into five groups, which differ in subunit assembly, cofactor composition, redox partners and cellular location [2,35]. Although all of these enzymes are involved in hydrogen cycling, their physiological functions may vary considerably. In particular, (group 3) bidirectional hydrogenases, which are capable of catalyzing both hydrogen activation and evolution under physiological conditions, are able to bind (and convert) additional soluble substrates like coenzyme F_{420} [36,37] or NAD(P)(H) [38–40]. While most of these enzymes are found in *Archaea*, we will focus on bacterial NAD(H)-linked bidirectional hydrogenases [38]. NADP(H)-linked hydrogenases from hyperthermophilic *Archaea* [39–44] are not in the scope of this review as they differ substantially in terms of subunit arrangement and cofactor composition.

3.1. Modular structure and catalytic activities

In multimeric NAD(H)-linked [NiFe] hydrogenases, the large and small subunit are referred to as HoxH and HoxY, respectively. This HoxHY hydrogenase moiety is associated with an additional NADH:acceptor oxidoreductase (diaphorase) module, which couples the reversible cleavage of hydrogen to the oxidoreduction of NAD(H) (Fig. 1B). The catalytic reaction with NADP(H) yields much lower H_2 evolution and consumption rates, indicating that NAD(H) is indeed the preferred, native substrate of bidirectional [NiFe] hydrogenases [45]. This argumentation is also supported by the fact that the involved nucleotide binding site appears to repel the phosphate group of NADP(H) [46]. The diaphorase moiety consists of at least two subunits, HoxF and HoxU, which exhibit pronounced sequence similarity to the peripheral part of the respiratory Complex I as well as certain formate dehydrogenases and [FeFe] hydrogenases [46–52]. NAD(H)-linked hydrogenases can be further divided in two classes, which differ in subunit and cofactor composition as well as their specific physiological function. In "cyanobacterial type" bidirectional hydrogenases [50,51,53–55], which have also been reported for purple sulphur bacteria [56,57], the diaphorase moiety is associated with an additional HoxE subunit [50], which might be involved in membrane interactions [54,56] or the electronic coupling between the hydrogenase and diaphorase active sites [45]. This subunit is absent in a second group of bidirectional hydrogenases from aerobic bacteria, including those from the actinobacterium *Rhodococcus opacus* MR11 [58,59] and the β-proteobacterium *Ralstonia eutropha* H16 [38]. The bidirectional hydrogenase from the latter organism comprises an additional diaphorase-associated $HoxI_2$ dimer, which contains a putative nucleotide binding site similar to that of cAMP receptors [60]. In line with this observation, $HoxI_2$ has been reported to act as an alternative electron entry site for reductive activation through an NADPH binding site [60].

3.2. Physiological functions and applications in biotechnology

In cyanobacteria, bidirectional hydrogenases are mainly involved in the disposal of excess electrons derived from

fermentation and photosynthesis [61–63], resulting in hydrogen evolution. A general role in the substitution of missing subunits of respiratory Complex I appears rather unlikely, as the absence of a functional bidirectional hydrogenase has been reported to be not essential for cyanobacterial cell growth [53–55,64–66]. Bidirectional hydrogenases from aerobic bacteria, on the other hand, differ in their catalytic bias as they rather catalyze hydrogen splitting, i.a. to supply reducing equivalents (NADH) to Complex I, thereby establishing a proton motive force. By transhydrogenases, NADH is also converted to NADPH, which can be used for carbon fixation during autotrophic growth [67]. Furthermore, these enzymes can also function as an electron valve by catalyzing hydrogen evolution in case of over-reducing conditions, i.e., an excess of NADH in the cytoplasm [68,69]. While aerobic bidirectional hydrogenases are strictly located in the cytoplasm [38,59] both a cytoplasmic localization [70] and a weak association with the cytoplasmic [71] or thylakoid [72] membrane has been suggested for cyanobacterial hydrogenases.

NAD(H)-linked bidirectional hydrogenases are of particular interest for biotechnological applications as they are suited for light driven hydrogen production in vivo [73] and the regeneration of reduced purine nucleotides in biocatalytic processes [74–79]. Such applications are particularly promising as some of these enzymes are oxygen tolerant [38,58,80–82], in contrast to most other hydrogenases.

4. Structure–function relationships in bidirectional hydrogenases

NAD(H)-linked bidirectional hydrogenases are complex multicofactor enzymes. Regarding subunit composition and cofactor content, these enzymes differ considerably from other hydrogenases, including "standard" [NiFe] hydrogenases (Fig. 1A and B). Unfortunately, there is no crystal structure available for a bidirectional hydrogenase so far, such that structural information about these enzymes has to rely on spectroscopic studies and comparison with related enzymes. Three major types of redox active cofactors are present in this class of enzymes: a [NiFe] active site, several Fe–S clusters, and one or two non-covalently bound flavins (see Table 1). Interestingly, [4Fe–4S] clusters of bidirectional hydrogenases exhibit lower midpoint potentials (about −450 mV) compared to those in "standard" [NiFe] hydrogenases (about −340 mV) [83–87]. In line with this finding, reductive (re-)activation of bidirectional hydrogenases requires low-potential electrons from NAD(P)H [60,80,88,89] and, thus, a lower switch-on potential E_{switch} is observed [90,91]. Within the evolutionary context, these observations can be explained by the fact that bidirectional hydrogenases interact with the low-potential NAD(H) pool while "standard" [NiFe] hydrogenases are rather linked to the higher-potential quinone pool of the respiratory chain in vivo [38,60,92].

4.1. The hydrogen converting active site

Also in bidirectional [NiFe] hydrogenases, hydrogen conversion takes place at a conserved [NiFe] center, which is located in the HoxH subunit of the hydrogenase sub-complex HoxHY. In contrast to other [NiFe] hydrogenases, however, no or only sub-stoichiometric amounts of paramagnetic Ni(III) species have been detected in most EPR studies on purified bidirectional hydrogenases [80,84,89,93–96]. This observation was taken as an indication for a different catalytic cycle where Ni remains in the diamagnetic Ni(II) state [96]. Alternatively, magnetic coupling between the Ni site and a second nearby paramagnetic center might prevent the detection of paramagnetic Ni(III) species under most conditions [93]. The enrichment of certain paramagnetic species might also be hampered for thermodynamic or kinetic reasons in this type of enzyme. However, for the bidirectional hydrogenase from *R. eutropha*, a quantitative EPR detection of the paramagnetic Ni_a-C state has been reported for a narrow potential range [83], indicating that monitoring of Ni(III) species in bidirectional hydrogenases might be strongly dependent on the adjustment of adequate experimental conditions [88], as also observed for Hydrogenase I from the archaeon *Pyrococcus furiosus* [97].

Table 1
Subunit composition and cofactor content of NAD(H)-linked bidirectional [NiFe] hydrogenases in comparison to the homologous parts of Complex I.

Bidirectional hydrogenase		Complex I homologue		Comment	References
Subunit	Cofactor	Subunit	Cofactor		
HoxH	[NiFe]	Nqo4	–	Binding motif conserved in all [NiFe] hydrogenases	[11]
HoxY	[4Fe–4S]	Nqo6	[4Fe–4S] (N2)	Corresponds to the proximal cluster in "standard" [NiFe] hydrogenases	[10,11,46,49–51,53,57,98,99]
	FMN-a		–	Reported only for *R. eutropha* SH, flavodoxin-like binding fold conserved in all [NiFe] hydrogenases and Complex I, has been proposed to occur in Complex I as well	[8,10,49,99,107,111,114]
HoxU	[4Fe–4S] (or [3Fe–4S])	Nqo3	[4Fe–4S] (N5)	3Cys-1His-coordinated [4Fe4S] cluster in Complex I, might be a 3Cys-coordinated [3Fe4S] cluster in some bidirectional hydrogenases, corresponds to the proximal cluster of [FeFe] hydrogenase	[6,10,53,57,90,105]
	[4Fe–4S]		–	Corresponds to the medial cluster of [FeFe] hydrogenase, part of a 2[4Fe–4S] motif, not in Nqo3 of Complex I (binding motif conserved) and HoxU from *R. eutropha*/*R. opacus*	[6,10,53,57,69,104,105]
	[4Fe–4S]		[4Fe–4S] (N4)	Corresponds to the distal cluster in [FeFe] hydrogenase, part of a 2[4Fe–4S] motif	[6,10,53,57,69,104,105]
	[2Fe–2S]		[2Fe–2S] (N1b)	Binding motif conserved in [FeFe] hydrogenase from *C. pasterianum*	[6,10,53,57,105]
HoxF	[4Fe–4S]	Nqo1	[4Fe4S] (N3)	Fe–S cluster closest to the NADH binding site of Complex I and (supposedly) bidirectional hydrogenases	[10,46,51,53,57]
	FMN-b		FMN	Non-classical Rossman fold binds both FMN and NADH in Complex I	[46,51,53,57,98]
	[2Fe–2S]	Nqo2	[2Fe–2S] (N1a)	Binding motif conserved in [FeFe] hydrogenase from *D. fructosovorans*, not in HoxF from *R. eutropha* and *R. opacus*	[50,57,104]
HoxE	[2Fe–2S]	Nqo2	[2Fe–2S] (N1a)	Binding motif conserved in [FeFe] hydrogenase from *D. fructosovorans*, HoxE missing in *R. eutropha* and *R. opacus* as well as Hox2 from *Thiocapsa roseopersicina*	[50,57,104,125]
HoxI	–	–	–	Reported only for *R. eutropha* SH, homology to cAMP receptors	[60,69]

Active sites of a few bidirectional hydrogenases have also been characterized by IR spectroscopy: At least four different redox states have been identified for the bidirectional hydrogenase from the cyanobacterium *Synechocystis* sp. PCC6803 (Fig. 3). An oxidized and a reduced species appeared to be EPR-silent (*vide supra*), while two transitional states were just observed during re-oxidation of the enzyme. Therefore, no EPR-data are available for the latter two, one of which might correspond to the Ni_a-C state of standard [NiFe] hydrogenases [89]. All of these different redox states exhibit one CO and two CN stretching bands in the IR spectrum, indicating a standard set of inorganic ligands at the active site. Moreover, most of these species display ligand stretching frequencies comparable to other [NiFe] hydrogenases, which suggests a similar (electronic) structure of the active site. However, the "fully" reduced state exhibits an unusually high CO stretching frequency in this enzyme (*vide infra*). Preliminary IR data from the HoxHY hydrogenase subcomplex of the cyanobacterial type bidirectional hydrogenase from *Allochromatium vinosum* revealed a mixture of states, with some of them resembling those of the hydrogenase from *Synechocystis* sp. [57]. For the bidirectional hydrogenase from *R. eutropha* EPR and IR properties of the active site have been discussed controversially and will be presented in more detail in Section 5.

Interestingly, (spectro-)electrochemical studies on bidirectional hydrogenases from *R. eutropha* and *Synechocystis* sp. indicate that the formation of the respective highest oxidized state might be dependent on the presence of oxygen [91,96]. This suggests that these redox species could possibly contain a bridging ligand other than OH^-, as this chemical species can also be derived anaerobically from water. Alternatively, the formation of the fully oxidized state might be kinetically unfavorable by electrochemical means, as observed for Ni_r-B formation in certain "standard" [NiFe] hydrogenases [17,25]. For the above mentioned bidirectional enzymes, protein film voltammetry and IR spectroscopy also revealed the occurrence of one or two additional oxidized states, which might, however, be related to non-native species that possibly arise from changes in the quaternary structure of the enzyme, e.g., the absence of the diaphorase moiety [90,91].

4.2. Iron sulphur clusters

By sequence analysis, the presence of up to eight Fe–S clusters has been predicted for NAD(H)-linked bidirectional hydrogenases [46,49–51,53,57,98,99] (Table 1). For all characterized enzymes, at least one [2Fe–2S] and one [4Fe–4S] cluster have been detected by EPR spectroscopy [80,83,84,89,93–96]. Sub-stoichiometric signals reminiscent of [3Fe–4S] clusters were also observed in these studies, but largely ascribed to oxidative damage or higher oxidation states of low potential [4Fe–4S] clusters. This interpretation is in agreement with the absence of [3Fe–4S] clusters in Complex I and [FeFe] hydrogenases [6,10]. Nonetheless, experimental insights indicate that functional [3Fe–4S] clusters may appear in certain bidirectional hydrogenases [94].

For the hydrogenase sub-complex HoxHY, sequence analysis indicates the presence of a single proximal [4Fe–4S] cluster in the HoxY subunit of bidirectional hydrogenases (Fig. 1) [46,49–51,53,57,98,99]. This binding motif is conserved among all [NiFe] hydrogenases and the Nqo6 subunit of Complex I (cluster N2) [11]. In fact, EPR, UV/vis, Mössbauer, and/or XAS studies on the separate HoxHY moieties from *R. eutropha* [90], *R. opacus* [93,94], and *A. vinosum* [57] indicate the presence of a [4Fe–4S] cluster in this sub-complex. For the sake of completeness, it should be mentioned that early studies claimed a location in the large HoxH subunit for this cubane cluster [94,100,101]. However, this appears unlikely as no conserved Fe–S cluster binding motif is present in HoxH of [NiFe] hydrogenases and the homologous Nqo4 subunit of Complex I [11]. The absence of the medial [3Fe–4S] and the distal [4Fe–4S] cluster, present in "standard" [NiFe] hydrogenases, can be explained by the fact that the small subunit (HoxY) is truncated at the C-terminus of the polypeptide chain in bidirectional hydrogenases [11,51,98]. This indicates that the electronic coupling with the diaphorase moiety is presumably accomplished by the single [4Fe–4S] cluster while missing parts of HoxY might be functionally substituted by HoxU. The [NiFe] site in HoxH and the [4Fe–4S] cluster in HoxY appear to represent the minimum set of cofactors necessary for hydrogen conversion in [NiFe] hydrogenases [57,90,93].

Interestingly, the HoxY-linked [4Fe–4S] cluster appeared to be EPR-silent, but was detected by XAS in a study on the separate HoxHY moiety of the bidirectional hydrogenase from *R. eutropha* [90], possibly indicating a magnetic coupling of this cofactor with another paramagnetic site. Studies on the separate hydrogenase modules from *R. opacus* [93,94] and *R. eutropha* [90] also revealed that this "proximal" cluster is particularly sensitive towards oxidation, as shown by irreversible conversion to a [3Fe–4S] and a [4Fe–nS–nO] cluster, respectively. This effect, however, might be at least partly related to the lack of the stabilizing diaphorase moiety. A structural rearrangement of the hydrogenase sub-complex in the absence of the diaphorase moiety is also indicated by the detection of two conformers of this "proximal" [4Fe–4S] cluster in HoxHY from *R. opacus* [94]. Only one of these conformers was also detected in the native tetrameric enzyme HoxHYFU, while the second was reported to be a less active structural variant.

For the diaphorase module, a precise characterization of the individual Fe–S clusters is more intricate for three major reasons. First of all, this moiety contains a large number of potential binding sites for Fe–S clusters, which complicates their respective quantification and assignment. Secondly, spectroscopic studies on the separate diaphorase moiety of a bidirectional hydrogenase have only been published for the enzyme from *R. opacus* [93,94] and, thus, most assumptions on Fe–S cluster location and function are deduced from sequence analysis and comparison with the homologous subunits of respiratory Complex I (Fig. 1B and C). Finally, the content of both proposed and detected Fe–S clusters is different in cyanobacterial and aerobic bidirectional hydrogenases, which might be related to their different physiological roles.

For bidirectional hydrogenases from aerobic bacteria, the presence of Fe–S clusters in the diaphorase module was derived from EPR and Mössbauer studies [80,83,84,93,94,96], revealing one [2Fe–2S] and two [4Fe–4S] clusters. Based on investigations of the separate HoxFU moiety from *R. opacus* [94], an additional, seemingly native [3Fe–4S] cluster has been reported for this particular enzyme. Interestingly, stoichiometric signals of this [3Fe–4S] cluster have only been observed in the isolated HoxFU module, while the native *R. opacus* enzyme exhibits a broad $g = 1.95$ signal instead. This feature might be related to magnetic coupling of the [3Fe–4S] cluster with a nearby paramagnetic species such as the Ni atom of the active site or other so far undetected metal ions [94]. In conclusion, the presence of a [3Fe–4S] cluster can not be completely ruled out for certain bidirectional hydrogenases, in particular, since minor amounts of a comparable broadened feature at $g \sim 1.92$ have also been observed for the bidirectional [NiFe] hydrogenase from *R. eutropha* at 12 K [84]. Interestingly, a possible role in oxygen radical scavenging has been proposed for the medial [3Fe–4S] cluster of "standard" [NiFe] hydrogenases [48]. Considering superoxide production by bidirectional hydrogenases [52,102,103], a putative [3Fe–4S] cluster could have a similar function in this type of enzymes.

For cyanobacterial bidirectional hydrogenases, no studies on separate diaphorase modules are available so far. Investigations of entire enzymes revealed the presence of [2Fe–2S] and [4Fe–4S] clusters, both with a stoichiometry of ~1 spin per molecule [89,95]. As the presence of a [4Fe–4S] cluster has been confirmed

for the hydrogenase sub-complex, only signals of a [2Fe–2S] cluster can be unambiguously assigned to the diaphorase moiety. This is in sharp contrast to the prediction of up to seven Fe–S clusters for the diaphorase moiety of these enzymes (*vide infra*) [51,53].

Apart from experimental investigations, further valuable information on possible locations and functions of Fe–S clusters of the diaphorase moiety can be deduced from comparison with subunits from Complex I and other similar enzymes (Fig. 1B and C, Table 1). A conserved binding site for a single [2Fe–2S] cluster is observed in HoxE of cyanobacterial type bidirectional hydrogenases and the homologous Nqo2 and HndA subunits of Complex I and the *Desulfovibrio fructosovorans* [FeFe] hydrogenase, respectively [50,57,104]. Since the presence of this cluster (N1a) has been proven for Nqo2 [10], its occurrence in HoxE is anticipated, as well. In bidirectional hydrogenases, a specific role in electron transfer interactions with membrane components or the hydrogenase module has been suggested for this binuclear Fe–S center [45,56]. No Fe–S cluster binding motifs are present in the additional HoxI subunits of the bidirectional hydrogenase from *R. eutropha* [69].

HoxF can be described as a fusion protein from homologues of Nqo1 and Nqo2 of Complex I [46]. Furthermore, this subunit is homologous to the HndA gene product of the NADP-reducing [FeFe] hydrogenase from *D. fructosovorans* [104]. Apart from binding sites for FMN and NAD(H), this subunit harbors a [4Fe–4S] cluster binding motif, which corresponds to cluster N3 of Complex I [10,46,51,53,57]. In cyanobacterial bidirectional hydrogenases, the presence of an additional ferredoxin-like [2Fe–2S] cluster is indicated by a further binding site in HoxF [50,57]. In Complex I, cluster N1a has been suggested to act as an electron storage, thereby minimizing the production of reactive oxygen species [10]. Thus, binuclear Fe–S clusters in HoxE and/or HoxF might carry out similar functions in certain bidirectional hydrogenases. However, these [2Fe–2S] clusters are absent in oxygen tolerant bidirectional hydrogenases from aerobic bacteria, suggesting different oxygen protection strategies in these latter enzymes.

HoxU has a sequence similar to the N-terminal part of Nqo3 from Complex I as well as [FeFe] hydrogenases [46–49,53,57,104,105]. These conserved sequence stretches contain another ferredoxin-like binding motif for a [2Fe–2S] cluster, which corresponds to N1b of Complex I [53,57]. In addition, a ferredoxin-type 2[4Fe–4S] motif is found in HoxU of cyanobacterial bidirectional hydrogenases [53,57], in [FeFe] hydrogenases [6104,105], and Complex I [10]. While both of these cubane clusters have been detected in the *Clostridium pasterianum* [FeFe] hydrogenase [6], only one [4Fe–4S] cluster is present in the homologous binding fold of Complex I (cluster N4) [10]. In bidirectional hydrogenases from aerobic bacteria, only four out of the eight cysteine residues of this sequence motif are conserved in HoxU, indicating the presence of a single [4Fe–4S] cluster [57,69]. Furthermore, HoxU contains another sequence motif consisting of one histidine and three cysteine residues [53,57]. This conserved fold suggests the binding of another cubane cluster, as observed in Complex I (N5) and [FeFe] hydrogenases [6,10]. Alternatively, the cysteine residues of this sequence motif might coordinate a [3Fe–4S] cluster as reported in a combined EPR and Mössbauer study on the *R. opacus* hydrogenase [94]. According to this assumption, the number of experimentally detected and predicted Fe–S clusters would coincide in aerobic bidirectional hydrogenases, and trinuclear and tetranuclear Fe–S clusters in HoxU could possibly substitute those missing in HoxY, thereby preserving a standard-like electron relay (*vide supra*).

Apart from the detailed characterization of the individual clusters, two general questions arise from previous studies on Fe–S cofactors in bidirectional hydrogenases. The first one refers to the discrepancy between the number of potential binding motifs and EPR-detected Fe–S clusters, especially in cyanobacterial hydrogenases, which is neither reported for most other hydrogenases nor for Complex I. This situation might be related to the presence of Fe–S clusters, which are EPR silent due to magnetic coupling to other paramagnetic species in close vicinity. In addition, the detection of some Fe–S clusters might also be hampered under standard experimental conditions for thermodynamic or kinetic reasons, as suggested for individual clusters of Complex I [106]. Alternatively, the Fe–S cluster content might be underestimated due to an overestimation of the protein concentration [107]. More recent studies, however, rather indicate an underestimation of the protein concentration for the bidirectional hydrogenase from *Synechocystis* sp. [89]. Finally, it can not be excluded that some of the potential binding sites are simply not occupied by intact Fe–S clusters in some native or isolated enzymes.

The second major question refers to the functional role of the large number of Fe–S clusters detected and/or predicted in bidirectional hydrogenases. This peculiarity might be related to a branched electron transfer pathway, as indicated by the presence of putative alternative electron access sites in HoxE and $HoxI_2$ [56,60]. Alternatively, a large number of electron transfer units might be necessary in case of different electron pathways in hydrogen activation and evolution, as claimed for the bidirectional hydrogenase from *R. eutropha* [108]. Another possible explanation can be derived from EPR studies on Complex I, which indicate complex electron occupancy patterns and alternating redox potentials for the Fe–S clusters of this enzyme [106,109]. This property has been suggested to play a major role in the fast and energy efficient electron transfer of Complex I in vivo. A similar mechanism, which obviously depends on a sufficient set of Fe–S centers, might also exist in the related bidirectional hydrogenases. As stated above, individual clusters might also minimize superoxide production or perform other functions beyond basic electron transfer. Eventually, it can not be excluded that certain Fe–S clusters might simply stabilize the protein matrix or represent evolutionary remnants, as suggested for cluster N7 in Complex I [10].

4.3. Flavin cofactors

At least one flavin mononucleotide (FMN) has been detected in all examined NAD(H)-linked bidirectional hydrogenases [38,83,89,95,110]. Based on sequence homology with the Nqo1 subunit of Complex I [46,51,53,57,98] and spectroscopic investigations of the separate HoxFU moiety from *R. opacus* [93], this component is accepted to be located in the HoxF subunit of the diaphorase moiety (Fig. 1B and C, Table 1). Among hydrogenases, flavin cofactors have only been reported for NAD(P)(H)-linked enzymes (see also [97,104,111]), indicating their involvement in the redox conversion of purine nucleotides. In fact, FMN is known to act as a communicator between one-electron centers (Fe–S clusters) and two-electron centers (NADH) in Complex I [112], which suggests an analogous role in bidirectional hydrogenases. The X-ray structure of the peripheral domain of *Thermus thermophilus* Complex I shows that NADH is stacked next to the FMN cofactor of Nqo1 in an orientation appropriate for direct hydride transfer. This NADH binding site is conserved in HoxF [10,46,51,53,57,98], indicating that NADH oxidation most likely progresses in the same way. Furthermore, the separate HoxF subunit of *R. eutropha* has been claimed to exhibit diaphorase activity [113], which supports its affiliation with FMN and NAD(H) binding.

Apart from the active site flavin in HoxF (FMN-b), a second loosely bound FMN cofactor (FMN-a) has been detected in the bidirectional soluble hydrogenase from *R. eutropha* (SH) [107,110,114]. This cofactor is supposed to be located in the HoxY subunit of the hydrogenase sub-complex HoxHY [99,107,114], which is supported by the structural homology between this subunit and the FMN binding site of flavodoxin (Fig. 1B) [8]. This po-

tential FMN binding fold is conserved in all [NiFe] hydrogenases and the Nqo6 subunit of Complex I [8,99] (see Table 1). Therefore, the presence of a second FMN molecule has also been proposed for the latter enzyme [49,99,107]. However, flavin binding at this position has not been observed in Complex I or hydrogenases other than the SH. In standard [NiFe] hydrogenases, this might be due to limited space related to the presence of the medial and distal Fe–S cluster [99]. In other bidirectional hydrogenases, however, FMN-a might be simply released during purification, as indicated by its loose binding in *R. eutropha* [114]. In fact, recent studies have shown that this cofactor occurs only in sub-stoichiometric amounts in the isolated HoxHY sub-complex of *R. eutropha* [90], providing further evidence for the stabilizing role of the diaphorase moiety. In agreement with this observation, previous reports on the SH claimed that the loss of FMN-a under reducing conditions is accompanied by a reversible unfolding of the entire enzyme [114]. Since the association of the HoxHY and HoxFU moieties has been reported to be weaker in other bidirectional hydrogenases [57,93], a loss of this flavin compound is likely to occur in these enzymes. Alternatively, the lower amount of observable FMN in other bidirectional hydrogenases might also be related to a general tendency towards overestimated protein concentrations in enzymes containing an NADH:acceptor oxidoreductase module [107]. However, since there is no experimental evidence for a second FMN in these enzymes so far, it can not be excluded that the FMN-a compound is a unique feature of the bidirectional hydrogenase from *R. eutropha*.

Several functions have been proposed for this second FMN of the SH, which has been reported to be essential for the proper functionality and integrity of the enzyme [90,110,114]. As stated above, FMN is able to act as a two-to-one electron converter, which might also transfer electrons between the hydride evolving during hydrogen cleavage and the proximal [4Fe-4S] cluster [114]. Furthermore, it is possibly involved in the fast removal of oxygen species from the active site [90,114] and might, thus, contribute to the oxygen tolerance of this enzyme. Recent studies also indicate that this flavin cofactor might be important for the stability of the HoxHY sub-complex of the SH and its interaction with hydrogen [90].

An assured determination of the function(s) of FMN-a, however, is complicated by the fact that the binding sites of FMN-a and the proximal [4Fe-4S] cluster are spatially overlapping in the small subunit of "standard" [NiFe] hydrogenases [8] and, as a consequence, the exact location of these two cofactors can not be assigned unambiguously for the SH. Thus, it remains open whether these redox sites are arranged sequentially and, if so, which of these is in direct contact with the [NiFe] center. Since both binding sites have a similar distance to the active site in "standard" [NiFe] hydrogenases [8], a simple sequential arrangement is less likely, which suggests a functional role beyond basic electron transfer for the flavin cofactor in HoxY. Furthermore, the overlap of the FMN-a locus with the binding site of the [4Fe-4S] cluster might partly account for the observed unusual EPR properties of this cluster and the [NiFe] site as well as the easy release of the FMN compound from HoxY.

5. The soluble hydrogenase from *Ralstonia eutropha*: a unique oxygen tolerant biocatalyst

In the following, we will provide a more detailed overview on unique features of the NAD(H)-linked bidirectional [NiFe] hydrogenase from *R. eutropha* H16. *R. eutropha* is a "Knallgas" bacterium, harboring at least three different hydrogenases: a membrane bound uptake hydrogenase (MBH), a cytoplasmic regulatory hydrogenase (RH), and the NAD(H)-linked soluble hydrogenase (SH) [69]. In principle, there are two major reasons for the special interest in this particular bidirectional enzyme. First of all, *R. eutropha* is a facultative chemolitoautotroph which is able to grow in the presence of oxygen by using H_2 and CO_2 as the sole electron and carbon source, respectively [67]. As a consequence, all three hydrogenases purified from this organism are able to catalyze hydrogen conversion in the presence of oxygen, which is in contrast to most other hydrogenases [69,92]. For the RH, this property has been ascribed to a narrowed gas channel, which limits oxygen access to the active site [15,115]. In the MBH, an unusual proximal Fe–S cluster has been recently reported to prevent the formation of the inactive Ni_u-A state by supplying electrons at high potentials [116]. In case of the SH, a modified active site has been previously suggested to play a role in its oxygen tolerance, however, this has been recently disproven (*vide infra*) [80–82,88]. Its tolerance towards oxygen renders the SH an outstanding biocatalyst for potential biotechnological applications, in particular, since this enzyme preferentially catalyzes the production of NADH rather than its oxidation. Therefore, the SH is particularly suited for the in situ regeneration of NADH in coupled enzymatic reactions [74,76–79]. Moreover, this enzyme has been extensively studied for more than three decades and, as a consequence, it represents the best characterized bidirectional hydrogenase and an established model system for this type of enzymes.

Like other bidirectional hydrogenases, the SH consists of the hydrogenase (HoxHY) and diaphorase (HoxFU) moieties, expanded by the aforementioned $HoxI_2$ homodimer [60]. The putative content, localization and function of Fe–S clusters and flavin compounds, including the unprecedented FMN-a in HoxY [114], have already been discussed for this enzyme (*vide supra*). In the following paragraphs, we will mainly focus on the unusual spectroscopic properties of the [NiFe] active site and its putative structural and functional peculiarities.

5.1. The active site of the soluble hydrogenase: the previous model and its shortcomings

As mentioned above, spectroscopic and structural features of the SH have been discussed controversially for more than a decade. Thus, we will present the previous structural and functional model for this enzyme first before discussing several objections and contradictory results from recent in situ studies (Section 5.2).

In standard [NiFe] hydrogenases, the $Fe(CO)(CN)_2$ moiety of the active site gives rise to three distinct infrared absorptions, which correspond to the carbonyl stretching vibration ν(CO) and the symmetric and antisymmetric stretching modes ν_s(CN) and ν_{as}(CN) of the two vibrationally coupled cyanide ligands [12,13]. Due to the π-acceptor and σ-donor capabilities of the CO and CN^- ligands, the frequencies of these vibrations are sensitive towards changes in the structure and redox state of the active site [9,12,117,118]. In contrast to standard [NiFe] hydrogenases, the IR spectrum of the as-isolated, oxidized SH exhibits one CO and four instead of two CN absorptions. Based on this observation and a chemical cyanide determination, the presence of two additional cyanide ligands was suggested for the active site of this enzyme (Fig. 4A) [80,81], which is, however, in sharp contrast to recent studies (*vide infra*) [88,90]. The frequencies of the CO and three of the four CN stretching modes were found to be insensitive towards redox state changes of the enzyme [80,81,96]. Consequently, these bands were assigned to a $Fe(CO)(CN)_3$ moiety, which does not undergo redox-dependent changes [80]. Only one of the CN stretching modes, detected at 2098 cm^{-1} for the oxidized enzyme, was reported to shift towards lower wavenumbers under reducing conditions. As a consequence, it was argued that the CN^- ligand reflected by this absorption was not coordinated to the same metal atom as the CO ligand, but rather bound to Ni (Fig. 4A) [80]. Since this 2098 cm^{-1} band was absent in the spectrum of SH puri-

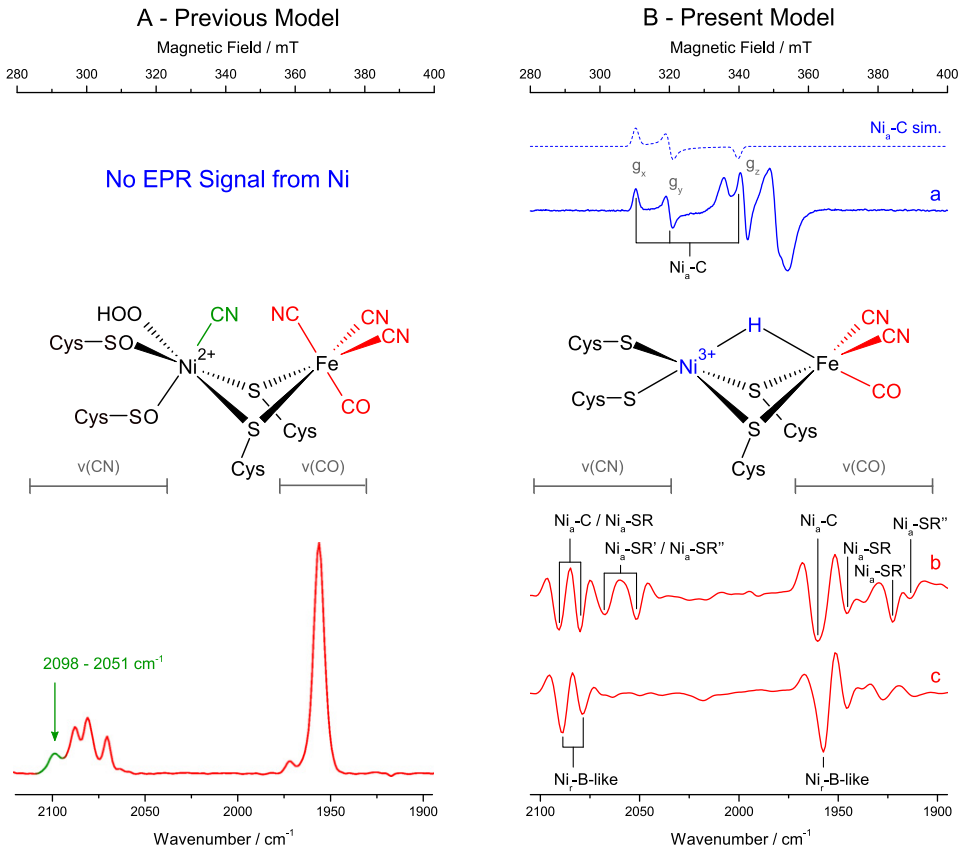

Fig. 4. Previous (A) and present (B) model for the active site structure of the soluble hydrogenase from *R.eutropha*. (A) Previous model derived from spectroscopic studies on the isolated enzyme [96] with the corresponding IR spectrum and the proposed structure of the fully oxidized enzyme displayed as a cartoon. For details, see text. (B) Summarized results from in vivo and in situ spectroscopic studies on the soluble hydrogenase from *R. eutropha* [88]. In living cells, about 60% of the enzyme resides in the paramagnetic Ni_a-C state (trace a), which can be converted to more oxidized or reduced EPR-silent Ni(II) species. In agreement with the reducing conditions within the cytoplasm, the second derivative of the IR spectrum from the same sample exhibits a mixture of "standard-like" reduced states with a predominant contribution from Ni_a-C (trace b). Under oxidizing conditions, an almost pure (EPR-silent) "Ni_r-B-like" state of the enzyme is represented by one CO and two CN stretching bands in the second derivative of the IR spectrum (trace c), indicating a standard set of inorganic ligands at the active site. The cartoon shows the present model for the active site structure of the native soluble hydrogenase in the Ni_a-C state.

fied from a Δ*hypX* deletion mutant, the HypX protein was claimed to be responsible for the incorporation of the proposed Ni-bound cyanide [82]. Furthermore, the presence and intensity of the 2098 cm^{-1} band was reported to correlate with the catalytic activity of the SH under aerobic conditions and, thus, the putative Ni-bound cyanide was suggested to play a major role in the oxygen tolerance of this enzyme by shielding the active site from oxygen [80–82]. In contrast to other [NiFe] hydrogenases, Ni-edge XAS investigations of the SH indicated the presence of a six-coordinate Ni atom, including hard ligand atoms like C, O, or N, especially in the fully oxidized state of the enzyme [108,119–121]. These observations were ascribed to sulfoxygenation at the terminal cysteinyl donors and a Ni-bound cyanide ligand (Fig. 4A). Furthermore, Ni-coordination by N/O atoms from water, amino side chains or amide groups of the protein backbone was proposed on the basis of these data.

As also observed for other bidirectional hydrogenases, no major contributions from paramagnetic Ni-species could be detected in most of the previous EPR studies on the SH [80,81,84,96]. As a consequence, the Ni atom has been suggested to remain unchanged in the Ni(II) state throughout the catalytic cycle [96,119]. Hydrogen cleavage was proposed to take place at a terminal coordination site of the Ni atom as the Fe atom was thought to be six-coordinate and, therefore, incapable of binding a bridging hydride. As the stretching frequencies of the putative $Fe(CO)(CN)_3$ moiety did not change under various conditions, all variations of the IR spectrum have been ascribed to a Ni-bound cyanide, reflecting changes in the number and type of Ni-coordinated ligands [80,81,96,119]. Based on these interpretations, the following model has been suggested for the catalytic cycle and the reductive activation of the SH active site [96,119]: In the oxidized state, the aerobically isolated SH exhibits one CO stretching at 1956 cm^{-1} and four CN stretchings at about 2098, 2090, 2080, and 2070 cm^{-1} (Fig. 4A). In this state, the enzyme is catalytically inactive and can not be readily activated by hydrogen. If substoichiometric amounts of NAD(P)H are added to the oxidized SH, the 2098 cm^{-1} band (assigned to the stretching mode of Ni-bound cyanide) disappears while intensity changes are observed for other CN stretching bands in the 2100–2050 cm^{-1} region. Based on band fitting analyses, these observations have been ascribed to a down-shift of the 2098 cm^{-1} band to ca. 2090 cm^{-1}, indicating a slight increase of electron density at the Ni-atom. This shift has been interpreted as a loss of a hydroxo or hydroperoxo species from Ni, which creates catalytically active SH with a vacant coordination site for hydride binding in a terminal position (Fig. 4A) [81]. When oxidized SH was incubated with both hydrogen and catalytic amounts of NAD(P)H, a new band was observed at 2051 cm^{-1}, which was again assigned to the stretching mode of Ni-bound cyanide, indicating a considerable increase of electron density at the Ni atom. This observation was tentatively ascribed to a displacement of the oxygen species by a terminally bound hydride. During catalysis, the active site was thought to cycle between the latter two states by transferring the Ni-bound hydride to the nearby FMN-a.

The studies described above provided a seemingly self-consistent model for the structure and catalytic mechanism of the SH active site. Nonetheless, there were ambiguities and open questions, which motivated further detailed investigations of this enzyme. First, the coordination of two additional cyanide ligands to the [NiFe] center would lead to a highly tense structure. In fact, preliminary quantum chemical calculations of model compounds for the proposed active site failed since the complex dissociated during geometry optimization.[b] Second, the disappearance of the ν(CN) = 2098 cm^{-1} band after incubation of the SH with sub-stoichiometric amounts of NAD(P)H has been assigned to a red shift ($\Delta\nu = -8$ cm^{-1}) of this absorption band [81]. This should lead to a defined absorbance increase at 2090 cm^{-1}, however, the experimental IR spectra exhibit relative intensity changes in the entire 2100–2050 cm^{-1} region, which indicates that the observed spectral changes are not related to a single ligand or exclusive changes at the Ni-atom. In addition, the terminal Ni-bound hydride ligand proposed for the fully reduced state of the enzyme should give rise to a well-defined ν(Ni−H) vibrational absorption in the spectral region between 2250 and 1700 cm^{-1} [122], as also predicted by spectra calculations on a [NiFe] site model compound.[2] However, no experimental evidence has been reported for this feature to date. Furthermore, IR studies on enzyme preparations enriched with ^{15}N by 50% were not conclusive [81]. This kind of experiment leads to three sets of ν(CN) bands reflecting enzyme populations with different degrees of ^{15}N labeling [13]. Molecules without ^{15}N labeled cyanide ligands show the usual ν(CN) band pattern while a complete labeling of all cyanide ligands shifts the entire ν(CN) signature towards lower wavenumbers. A third set of bands reflects 2^n-2 populations where only a part of the *n* cyanide ligands is labeled with ^{15}N. An active site with four cyanide ligands should give rise to 14 of these latter populations, which would, as a consequence, dominate the IR spectrum. Even if the Ni-bound cyanide was unaffected by partial ^{15}N labeling for metabolic reasons [81], still six of these populations should arise from the three Fe-bound cyanides. However, like in standard [NiFe] hydrogenases, only two medium strong bands arose from partial ^{15}N labeling, which is in contrast to the assumption of additional cyanide ligands at the SH active site. In addition, the model's assumption of a redox-inactive Ni(II) state during reductive activation and catalysis is in conflict with the detection of the paramagnetic Ni_a-C state for SH incubated with an excess of NADH [83]. These observations have been later ascribed to a loss of the additional cyanide ligands, which was suggested to render the active site an oxygen sensitive standard [NiFe] center [96,119]. However, NADH is a substrate of the SH, which can also be present in large amounts under in vivo conditions (*vide infra*). Furthermore, cyanide is known to be among the most tightly bound inorganic ligands, which is unlikely to easily (and selectively) dissociate from the deeply buried active site under mild reducing conditions. These objections are in line with the finding that excess NADH leads to a completely reversible reduction of the bidirectional hydrogenase from *Synechocystis* sp. [89]. A particularly puzzling implication of the previous model is the redox inactivity of both Ni and Fe, questioning the functional role of the complex [NiFe] site. Additional concerns refer to the proposed terminal hydride binding at the Ni site. This scenario would imply that hydrogen conversion does not take place *cis* or *trans* to a carbonyl ligand, which is in contrast to all other known hydrogenases. In this context, it should be mentioned that a *cis* or (preferentially) *trans* oriented ligand with both electron donating and withdrawing capabilities (like CO) is assumed to be essential for the reversible binding and cleavage of H_2, respectively [34]. Finally, the proposed involvement of the Ni-bound cyanide in the oxygen tolerance of the SH [96] is not convincing, since this ligand would only shield the bridging site between the two metals. However, a blocking of the bridging position by additional cyanide ligands would not sterically shield the terminal coordination site on the Ni, where hydrogen cycling was proposed to take place (Fig. 4A).

5.2. New insights from in vivo and in situ spectroscopy

Due to the shortcomings of the model discussed in the preceding section, the SH from *R. eutropha* has been recently reinvestigated in a combined approach using IR and EPR spectroscopy [88]. In contrast to former spectroscopic investigations on purified SH, this study has been performed on whole cells of an *R. eutropha* H16 wild type derivative that expresses no hydrogenases other than the SH. Thus, the enzyme could be characterized within its native cytoplasmic environment. Under in vivo conditions, i.e., within living cells, it was shown that the SH mainly exists in the paramagnetic Ni_a-C state, which is in agreement with its coupling to the cellular pool of reductants (Fig. 4B, trace a). As monitored by EPR spectroscopy, this Ni(III) species disappears under more reducing or oxidizing conditions, indicating a redox active Ni-atom in the native enzyme. In addition to the prevalent Ni_a-C state, complementary IR studies revealed a mixture of further redox states, as also observed in "standard" [NiFe] hydrogenases (Figs. 3 and 4B, trace b). These findings demonstrate that the SH active site contains a standard set of inorganic ligands, i.e., one CO and two CN^-. This conclusion has been further proven by the IR spectrum of a nearly pure EPR-silent oxidized state, exhibiting only one CO and two CN stretching modes, which resemble the IR signature of the Ni_r-B state in "standard" [NiFe] hydrogenases (Fig. 4B, trace c). Thus, the active site structure of the native SH is much more similar to standard [NiFe] hydrogenases and the previous model involving an unusual ligation pattern of the [NiFe] center can be discarded (Fig. 4B, cartoon).

In a more general sense, these studies indicate that a representative characterization of complex biological systems is strongly dependent on the preservation or recreation of native conditions. For the SH, quantitative amounts of the Ni_a-C state have only been observed within the cytoplasm of living cells [88] or, mimicking these reducing conditions, by adding excess amounts of NADH [83]. In agreement with previous suggestions [93,97], this finding indicates that a detection of paramagnetic Ni(III) species in bidirectional hydrogenases requires the careful selection of appropriate experimental conditions.

Apart from these general insights, the above in situ studies have revealed a further reduced species of the SH, termed Ni_a-SR2 (Fig. 3), which was also observed in the bidirectional hydrogenase from *Synechocystis* sp.[3] [88,89]. Compared to Ni_a-SR states observed in standard [NiFe] hydrogenases, this species exhibits an unusually high CO stretching frequency at 1958 cm^{-1}. Hence, this state could be a low potential Ni(III) species similar to Ni_a-C (ν(CO) = 1962 cm^{-1} in *R. eutropha*) or the putative Ni_a-X state of the oxidative addition mechanism, proposed recently for hydrogen cycling in [NiFe] hydrogenases [31]. This so far undetected Ni_a-X state has been described as an intermediate Ni(III) species with two hydride ligands at the active site, one in the bridging position between the two metals (like in Ni_a-C and Ni_a-SR) and one bound terminally to the sixth coordination site of the Ni atom. Such a species might exhibit spectral similarities to the detected Ni_a-SR2 state. However, preliminary calculations of IR spectra of a [NiFe] model compound suggest that the terminal hydride of Ni_a-X should give rise to a well defined ν(Ni−H) band in the 2000–1900 cm^{-1} region and a particularly low CO stretching frequency.[4] In addition, such a Ni(III) species

[2] M. Horch. Unpublished results.

[3] For the enzyme from *Synechocystis* sp., this species has been previously assigned to the Ni_a-SR state [89].

[4] M. Horch. Unpublished results.

should also display a prominent EPR signal, which has not been observed in the experiment. Therefore, Ni_a-SR2 may rather be a Ni(II) species where the ligand at the bridging site exerts a strong *trans* influence on the opposite CO ligand.[5] This effect should weaken the Fe–CO and strengthen the C≡O bond, thereby selectively increasing the frequency of the CO stretching mode, as observed for Ni_a-SR2. Possible candidates for such a scenario may be a H_2 σ-bond complex or related species facing the bridging site. In fact, a similar effect was also observed in the Ni_a-C state of "standard" [NiFe] hydrogenases, where the bridging hydride acts as a strong σ-donor *trans* to the CO ligand such that ν(CO) is indeed considerably increased [27].

6. Outlook: challenges for future research

Over the last three decades, spectroscopic and biochemical studies have provided considerable insights into functional aspects and structural determinants in NAD(H)-linked bidirectional hydrogenases. Despite notable scientific advances, however, there are still numerous questions to address in order to gain a comprehensive understanding of this type of enzymes. In particular, little is known about the function and interaction of the individual Fe-S clusters, especially in the diaphorase moiety. Another, closely related question arises from the finding that stoichiometric amounts of paramagnetic species of the active site and certain Fe-S clusters are difficult to detect. This observation may be related to unusual redox properties and pronounced magnetic interactions of the various cofactors. In terms of future applications, special attention has to be paid to the investigation of oxygen-tolerance mechanisms in certain bidirectional [NiFe] hydrogenases like the SH from *R. eutropha*. In this context, the supply of low-potential electrons from the oxidation of NAD(P)H appears to play a major role in preserving catalytic activity under aerobic conditions in vivo. However, despite considerable efforts and promising insights, the structural and mechanistic basis for this property has still to be resolved.

References

[1] Stephenson, M. and Stickland, L.H. (1931) Hydrogenase: a bacterial enzyme activating molecular hydrogen: the properties of the enzyme. Biochem. J. 25, 205–214.

[2] Vignais, P.M. and Billoud, B. (2007) Occurrence, classification, and biological function of hydrogenases: an overview. Chem. Rev. 107, 4206–4272.

[3] Lenz, O., Bernhard, M., Buhrke, T., Schwartz, E. and Friedrich, B. (2002) The hydrogen sensing apparatus in *Ralstonia eutropha*. J. Mol. Microbiol. Biotechnol. 4, 255–262.

[4] Buhrke, T., Lenz, O., Porthun, A. and Friedrich, B. (2004) The H_2-sensing complex of *Ralstonia eutropha*: interaction between a regulatory [NiFe] hydrogenase and a histidine protein kinase. Mol. Microbiol. 51, 1677–1689.

[5] Mertens, R. and Liese, A. (2004) Biotechnological applications of hydrogenases. Curr. Opin. Biotechnol. 15, 343–348.

[6] Peters, J.W., Lanzilotta, W.N., Lemon, B.J. and Seefeldt, L.C. (1998) X-ray crystal structure of the Fe-only hydrogenase (CpI) from *Clostridium pasteurianum* to 1.8 Ångstrom resolution. Science 282, 1853–1858.

[7] Shima, S., Pilak, O., Vogt, S., Schick, M., Stagni, M.S., Meyer-Klaucke, W., Warkentin, E., Thauer, R.K. and Ermler, U. (2008) The crystal structure of [Fe]-hydrogenase reveals the geometry of the active site. Science 321, 572–575.

[8] Volbeda, A., Charon, M.H., Piras, C., Hatchikian, E.C., Frey, M. and Fontecilla-Camps, J.C. (1995) Crystal structure of the nickel-iron hydrogenase from *Desulfovibrio gigas*. Nature 373, 580–587.

[9] Volbeda, A., Garcin, E., Piras, C., De Lacey, A.L., Fernandez, V.M., Hatchikian, E.C., Frey, M. and Fontecilla-Camps, J.C. (1996) Structure of the [NiFe] hydrogenase active site: evidence for biologically uncommon Fe ligands. J. Am. Chem. Soc. 118, 12989–12996.

[10] Sazanov, L.A. and Hinchliffe, P. (2006) Structure of the hydrophilic domain of respiratory Complex I from *Thermus thermophilus*. Science 311, 1430–1436.

[11] Albracht, S.P.J. (1993) Intimate relationships of the large and the small subunits of all nickel hydrogenases with two nuclear-encoded subunits of mitochondrial NADH: ubiquinone oxidoreductase. Biochim. Biophys. Acta 1144, 221–224.

[12] Happe, R.P., Roseboom, W., Pierik, A.J., Albracht, S.P.J. and Bagley, K.A. (1997) Biological activition of hydrogen. Nature 385, 126.

[13] Pierik, A.J., Roseboom, W., Happe, R.P., Bagley, K.A. and Albracht, S.P.J. (1999) Carbon monoxide and cyanide as intrinsic ligands to iron in the active site of [NiFe] hydrogenases. J. Biol. Chem. 274, 3331–3337.

[14] Volbeda, A. and Fontecilla-Camps, J.C. (2003) The active site and catalytic mechanism of NiFe hydrogenases. Dalton Trans. 21, 4030–4038.

[15] Volbeda, A., Montet, Y., Vernède, X., Hatchikian, E.C. and Fontecilla-Camps, J.C. (2002) High-resolution crystallographic analysis of *Desulfovibrio fructosovorans* [NiFe] hydrogenase. Int. J. Hydrogen Energy 27, 1449–1461.

[16] Montet, Y., Amara, P., Volbeda, A., Vernede, X., Hatchikian, E.C., Field, M.J., Frey, M. and Fontecilla-Camps, J.C. (1997) Gas access to the active site of Ni–Fe hydrogenases probed by X-ray crystallography and molecular dynamics. Nat. Struct. Mol. Biol. 4, 523–526.

[17] De Lacey, A.L., Hatchikian, E.C., Volbeda, A., Frey, M., Fontecilla-Camps, J.C. and Fernandez, V.M. (1997) Infrared-spectroelectrochemical characterization of the [NiFe] hydrogenase of *Desulfovibrio gigas*. J. Am. Chem. Soc. 119, 7181–7189.

[18] De Lacey, A.L., Fernandez, V.M., Rousset, M. and Cammack, R. (2007) Activation and inactivation of hydrogenase function and the catalytic cycle: spectroelectrochemical studies. Chem. Rev. 107, 4304–4330.

[19] van Gastel, M., Stein, M., Brecht, M., Schröder, O., Lendzian, F., Bittl, R., Ogata, H., Higuchi, Y. and Lubitz, W. (2006) A single-crystal ENDOR and density functional theory study of the oxidized states of the [NiFe] hydrogenase from *Desulfovibrio vulgaris* Miyazaki F. J. Biol. Inorg. Chem. 11, 41–51.

[20] Volbeda, A., Martin, L., Cavazza, C., Matho, Ml., Faber, B.W., Roseboom, W., Albracht, S.P.J., Garcin, E., Rousset, M. and Fontecilla-Camps, J.C. (2005) Structural differences between the ready and unready oxidized states of [NiFe] hydrogenases. J. Biol. Inorg. Chem. 10, 239–249.

[21] Fernandez, V.M., Hatchikian, E.C. and Cammack, R. (1985) Properties and reactivation of two different deactivated forms of *Desulfovibrio gigas* hydrogenase. Biochim. Biophys. Acta 832, 69–79.

[22] Ogata, H., Hirota, S., Nakahara, A., Komori, H., Shibata, N., Kato, T., Kano, K. and Higuchi, Y. (2005) Activation process of [NiFe] hydrogenase elucidated by high-resolution X-ray analyses: conversion of the ready to the unready state. Structure 13, 1635–1642.

[23] Coremans, J.M.C.C., van der Zwaan, J.W. and Albracht, S.P.J. (1992) Distinct redox behaviour of prosthetic groups in ready and unready hydrogenase from *Chromatium vinosum*. Biochim. Biophys. Acta 1119, 157–168.

[24] Lubitz, W., Reijerse, E. and van Gastel, M. (2007) [NiFe] and [FeFe] hydrogenases studied by advanced magnetic resonance techniques. Chem. Rev. 107, 4331–4365.

[25] Bleijlevens, B., van Broekhuizen, F.A., De Lacey, A.L., Roseboom, W., Fernandez, V.M. and Albracht, S.P.J. (2004) The activation of the [NiFe]-hydrogenase from *Allochromatium vinosum*. An infrared spectro-electrochemical study. J. Biol. Inorg. Chem. 9, 743–752.

[26] Brecht, M., van Gastel, M., Buhrke, T., Friedrich, B. and Lubitz, W. (2003) Direct detection of a hydrogen ligand in the [NiFe] center of the regulatory H_2-sensing hydrogenase from *Ralstonia eutropha* in its reduced state by HYSCORE and ENDOR spectroscopy. J. Am. Chem. Soc. 125, 13075–13083.

[27] Volbeda, A. and Fontecilla-Camps, J.C. (2005) Structure-function relationships of nickel-iron sites in hydrogenase and a comparison with the active sites of other nickel-iron enzymes. Coord. Chem. Rev. 249, 1609–1619.

[28] Fichtner, C., Laurich, C., Bothe, E. and Lubitz, W. (2006) Spectroelectrochemical characterization of the [NiFe] hydrogenase of *Desulfovibrio vulgaris* Miyazaki F. Biochemistry 45, 9706–9716.

[29] Ogata, H., Lubitz, W. and Higuchi, Y. (2009) Structural and spectroscopic studies of the reaction mechanism. Dalton Trans. 37, 7577–7587.

[30] van der Zwaan, J.W., Albracht, S.P.J., Fontijn, R.D. and Slater, E.C. (1985) Monovalent nickel in hydrogenase from *Chromatium vinosum*: light sensitivity and evidence for direct interaction with hydrogen. FEBS Lett. 179, 271–277.

[31] Lill, S.O.N. and Siegbahn, P.E.M. (2009) An autocatalytic mechanism for NiFe-hydrogenase: reduction to Ni(I) followed by oxidative addition. Biochemistry 48, 1056–1066.

[32] Siegbahn, P.E.M., Tye, J.W. and Hall, M.B. (2007) Computational studies of [NiFe] and [FeFe] hydrogenases. Chem. Rev. 107, 4414–4435.

[33] Pardo, A., de Lacey, A., Fernandez, V.M., Fan, H.J., Fan, Y. and Hall, M. (2006) Density functional study of the catalytic cycle of nickel-iron [NiFe] hydrogenases and the involvement of high-spin nickel(II). J. Biol. Inorg. Chem. 11, 286–306.

[34] Kubas, G.J. (2007) Fundamentals of H_2 binding and reactivity on transition metals underlying hydrogenase function and H_2 production and storage. Chem. Rev. 107, 4152–4205.

[35] Constant, P., Chowdhury, S.P., Hesse, L., Pratscher, J. and Conrad, R. (2011) Genome data mining and soil survey for the novel group 5 [NiFe]-hydrogenase to explore the diversity and ecological importance of presumptive high-affinity H_2-oxidizing bacteria. Appl. Environ. Microbiol. 77, 6027–6035.

[36] Fox, J.A., Livingston, D.J., Orme-Johnson, W.H. and Walsh, C.T. (1987) 8-Hydroxy-5-deazaflavin-reducing hydrogenase from *Methanobacterium thermoautotrophicum*: 1. Purification and characterization. Biochemistry 26, 4219–4227.

[5] A *trans* influence is observed, if two ligands are bound to a transition metal ion via the same orbital [123]. A pure σ-donor ligand (e.g. H^- or H_2) is expected to donate electron density to the d_z^2 orbital of the octahedral Fe center at the [NiFe] active site without interacting with occupied t_{2g} orbitals. This weakens σ-donation from the *trans* oriented CO ligand while π-backdonation remains virtually unaffected. As a consequence, ν(CO) is increased as described in the text.

[37] Muth, E., Mörschel, E. and Klein, A. (1987) Purification and characterization of an 8-hydroxy-5-deazaflavin-reducing hydrogenase from the archaebacterium *Methanococcus voltae*. Eur. J. Biochem. 169, 571–577.
[38] Schneider, K. and Schlegel, H.G. (1976) Purification and properties of soluble hydrogenase from *Alcaligenes eutrophus* H 16. Biochim. Biophys. Acta 452, 66–80.
[39] Ma, K., Hao, Z. and Adams, M.W.W. (1994) Hydrogen production from pyruvate by enzymes purified from the hyperthermophilic archaeon, *Pyrococcus furiosus*: a key role for NADPH. FEMS Microbiol. Lett. 122, 245–250.
[40] Bryant, F.O. and Adams, M.W. (1989) Characterization of hydrogenase from the hyperthermophilic archaebacterium, *Pyrococcus furiosus*. J. Biol. Chem. 264, 5070–5079.
[41] Ma, K., Weiss, R. and Adams, M.W.W. (2000) Characterization of hydrogenase II from the hyperthermophilic archaeon *Pyrococcus furiosus* and assessment of its role in sulfur reduction. J. Bacteriol. 182, 1864–1871.
[42] Ma, K., Schicho, R.N., Kelly, R.M. and Adams, M.W. (1993) Hydrogenase of the hyperthermophile *Pyrococcus furiosus* is an elemental sulfur reductase or sulfhydrogenase: evidence for a sulfur-reducing hydrogenase ancestor. Proc. Natl. Acad. Sci. USA 90, 5341–5344.
[43] Rakhely, G., Zhou, Z.H., Adams, M.W.W. and Kovacs, K.L. (1999) Biochemical and molecular characterization of the [NiFe] hydrogenase from the hyperthermophilic archaeon, *Thermococcus litoralis*. Eur. J. Biochem. 266, 1158–1165.
[44] Kanai, T., Ito, S. and Imanaka, T. (2003) Characterization of a cytosolic NiFe-hydrogenase from the hyperthermophilic archaeon *Thermococcus kodakaraensis* KOD1. J. Bacteriol. 185, 1705–1711.
[45] Aubert-Jousset, E., Cano, M., Guedeney, Gv., Richaud, P. and Cournac, L. (2011) Role of HoxE subunit in *Synechocystis* PCC6803 hydrogenase. FEBS J., DOI: 10.1111/j.1742-4658.2011.08308.x.
[46] Pilkington, S.J., Skehel, J.M., Gennis, R.B. and Walker, J.E. (1991) Relationship between mitochondrial NADH-ubiquinone reductase and a bacterial NAD-reducing hydrogenase. Biochemistry 30, 2166–2175.
[47] Patel, S.D., Aebersold, R. and Attardi, G. (1991) cDNA-derived amino acid sequence of the NADH-binding 51-kDa subunit of the bovine respiratory NADH dehydrogenase reveals striking similarities to a bacterial NAD(+)-reducing hydrogenase. Proc. Natl. Acad. Sci. USA 88, 4225–4229.
[48] Albracht, S.P.J. (1994) Nickel hydrogenases: in search of the active site. Biochim. Biophys. Acta 1188, 167–204.
[49] Albracht, S.P.J., Mariette, A. and de Jong, P. (1997) Bovine-heart NADH:ubiquinone oxidoreductase is a monomer with 8 Fe-S clusters and 2 FMN groups. Biochim. Biophys. Acta 1318, 92–106.
[50] Schmitz, O., Boison, G., Salzmann, H., Bothe, H., Schütz, K., Wang, Sh. and Happe, T. (2002) HoxE – a subunit specific for the pentameric bidirectional hydrogenase complex (HoxEFUYH) of cyanobacteria. Biochim. Biophys. Acta 1554, 66–74.
[51] Schmitz, O., Boison, G., Hilscher, R., Hundeshagen, B., Zimmer, W., Lottspeich, F. and Bothe, H. (1995) Molecular biological analysis of a bidirectional hydrogenase from cyanobacteria. Eur. J. Biochem. 233, 266–276.
[52] Lauterbach, L., Idris, Z., Vincent, K.A. and Lenz, O. (2011) Catalytic properties of the isolated diaphorase fragment of the NAD^+ -reducing [NiFe]-hydrogenase from *Ralstonia eutropha*. *PLoS ONE* 6, e25939.
[53] Appel, J. and Schulz, R. (1996) Sequence analysis of an operon of a NAD(P)-reducing nickel hydrogenase from the cyanobacterium *Synechocystis* sp. PCC 6803 gives additional evidence for direct coupling of the enzyme to NAD(P)H-dehydrogenase (Complex 1). Biochim. Biophys. Acta 1298, 141–147.
[54] Tamagnini, P., Leitao, E., Oliveira, P., Ferreira, D., Pinto, F., Harris, D.J., Heidorn, T. and Lindblad, P. (2007) Cyanobacterial hydrogenases: Diversity, regulation and applications. FEMS Microbiol. Rev. 31, 692–720.
[55] Tamagnini, P., Axelsson, R., Lindberg, P., Oxelfelt, F., Wunschiers, R. and Lindblad, P. (2002) Hydrogenases and hydrogen metabolism of cyanobacteria. Microbiol. Mol. Biol. Rev. 66, 1–20.
[56] Rakhely, G., Kovacs, A.T., Maroti, G., Fodor, B.D., Csanadi, G., Latinovics, D. and Kovacs, K.L. (2004) Cyanobacterial-type, heteropentameric, NAD^+-reducing NiFe hydrogenase in the purple sulfur photosynthetic bacterium *Thiocapsa roseopersicina*. Appl. Environ. Microbiol. 70, 722–728.
[57] Long, M., Liu, J., Chen, Z., Bleijlevens, B., Roseboom, W. and Albracht, S.P.J. (2007) Characterization of a HoxEFUYH type of [NiFe] hydrogenase from *Allochromatium vinosum* and some EPR and IR properties of the hydrogenase module. J. Biol. Inorg. Chem. 12, 62–78.
[58] Aggag, M. and Schlegel, H.G. (1973) Studies on a gram-positive hydrogen bacterium, *Nocardia opaca*; strain *1 b*. Arch. Microbiol. 88, 299–318.
[59] Schneider, K., Schlegel, H.G. and Jochim, K. (1984) Effect of nickel on activity and subunit composition of purified hydrogenase from *Nocardia opaca* 1b. Eur. J. Biochem. 138, 533–541.
[60] Burgdorf, T., van der Linden, E., Bernhard, M., Yin, Q.Y., Back, J.W., Hartog, A.F., Muijsers, A.O., de Koster, C.G., Albracht, S.P.J. and Friedrich, B. (2005) The soluble NAD^+-reducing [NiFe]-hydrogenase from *Ralstonia eutropha* H16 consists of six subunits and can be specifically activated by NADPH. J. Bacteriol. 187, 3122–3132.
[61] Appel, J., Phunpruch, S., Steinmüller, K. and Schulz, R. (2000) The bidirectional hydrogenase of *Synechocystis* sp. PCC 6803 works as an electron valve during photosynthesis. Arch. Microbiol. 173, 333–338.
[62] Stal, L.J. and Moezelaar, R. (1997) Fermentation in cyanobacteria. FEMS Microbiol. Rev. 21, 179–211.
[63] Troshina, O., Serebryakova, L., Sheremetieva, M. and Lindblad, P. (2002) Production of H_2 by the unicellular cyanobacterium *Gloeocapsa alpicola* CALU 743 during fermentation. Int. J. Hydrogen Energ. 27, 1283–1289.
[64] Schmitz, O. and Bothe, H. (1996) The diaphorase subunit HoxU of the bidirectional hydrogenase as electron transferring protein in cyanobacterial respiration? Naturwissenschaften 83, 525–527.
[65] Boison, G., Schmitz, O., Schmitz, B. and Bothe, H. (1998) Unusual gene arrangement of the bidirectional hydrogenase and functional analysis of its diaphorase subunit HoxU in respiration of the unicellular cyanobacterium *Anacystis nidulans*. Curr. Microbiol. 36, 253–258.
[66] Boison, G., Bothe, H., Hansel, A. and Lindblad, P. (1999) Evidence against a common use of the diaphorase subunits by the bidirectional hydrogenase and by the respiratory Complex I in cyanobacteria. FEMS Microbiol. Lett. 174, 159–165.
[67] Cramm, R. (2009) Genomic view of energy metabolism in *Ralstonia eutropha* H16. J. Mol. Microbiol. Biotechnol. 16, 38–52.
[68] Kuhn, M., Steinbuchel, A. and Schlegel, H.G. (1984) Hydrogen evolution by strictly aerobic hydrogen bacteria under anaerobic conditions. J. Bacteriol. 159, 633–639.
[69] Burgdorf, T., Lenz, O., Buhrke, T., van der Linden, E., Jones, A.K., Albracht, S.P.J. and Friedrich, B. (2005) [NiFe]-Hydrogenases of *Ralstonia eutropha* H16: modular enzymes for oxygen-tolerant biological hydrogen oxidation. J. Mol. Microbiol. Biotechnol. 10, 181–196.
[70] Hallenbeck, P.C. and Benemann, J.R. (1978) Characterization and partial purification of the reversible hydrogenase of *Anabaena cylindrica*. FEBS Lett. 94, 261–264.
[71] Kentemich, T., Bahnweg, M., Mayer, F. and Bothe, H. (2011) Localization of the reversible hydrogenase in cyanobacteria. Z. Naturforsch 44c, 384–391.
[72] Serebriakova, L., Zorin, N.A. and Lindblad, P. (1994) Reversible hydrogenase in *Anabaena variabilis* ATCC 29413. Arch. Microbiol. 161, 140–144.
[73] Prince, R.C. and Kheshgi, H.S. (2005) The photobiological production of hydrogen: potential efficiency and effectiveness as a renewable fuel. Cr. Rev. Microbiol. 31, 19–31.
[74] Okura, I., Otsuka, K., Nakada, N. and Hasumi, F. (1990) Regeneration of NADH and ketone hydrogenation by hydrogen with the combination of hydrogenase and alcohol dehydrogenase. Appl. Biochem. Biotechnol. 24–25, 425–430.
[75] Mertens, R., Greiner, L., van den Ban, E.C.D., Haaker, H.B.C.M. and Liese, A. (2003) Practical applications of hydrogenase I from *Pyrococcus furiosus* for NADPH generation and regeneration. J. Mol. Catal. B: Enzym. 24–25, 39–52.
[76] Payen, B., Segui, M., Monsan, P., Schneider, K., Friedrich, C.G. and Schlegel, H.G. (1983) Use of cytoplasmic hydrogenase from *Alcaligenes eutrophus* for NADH regeneration. Biotechnol. Lett. 5, 463–468.
[77] Cantet, J., Bergel, A., Comtat, M. and Séris, J.L. (1992) Kinetics of the catalysis by the *Alcaligenes eutrophus* H16 hydrogenase of the electrochemical reduction of NAD^+. J. Mol. Catal. 73, 371–380.
[78] Cantet, J., Bergel, A. and Comtat, M. (1992) Bioelectrocatalysis of NAD^+ reduction. J. Electroanal. Chem. 342, 475–486.
[79] Ratzka, J., Lauterbach, L., Lenz, O. and Ansorge-Schumacher, M.B. (2011) Systematic evaluation of the dihydrogen-oxidizing and NAD^+-reducing soluble [NiFe]-hydrogenase from *Ralstonia eutropha* as a cofactor regeneration catalyst. Biocat. Biotrans., DOI: 10.3109/10242422.2011.615393.
[80] Happe, R.P., Roseboom, W., Egert, G., Friedrich, C.G., Massanz, C., Friedrich, B. and Albracht, S.P.J. (2000) Unusual FTIR and EPR properties of the H_2-activating site of the cytoplasmic NAD-reducing hydrogenase from *Ralstonia eutropha*. FEBS Lett. 466, 259–263.
[81] van der Linden, E., Burgdorf, T., Bernhard, M., Bleijlevens, B., Friedrich, B. and Albracht, S.P.J. (2004) The soluble [NiFe]-hydrogenase from *Ralstonia eutropha* contains four cyanides in its active site, one of which is responsible for the insensitivity towards oxygen. J. Biol. Inorg. Chem. 9, 616–626.
[82] Bleijlevens, B., Buhrke, T., van der Linden, E., Friedrich, B. and Albracht, S.P.J. (2004) The auxiliary protein HypX provides oxygen tolerance to the soluble [NiFe]-hydrogenase of *Ralstonia eutropha* H16 by way of a cyanide ligand to nickel. J. Biol. Chem. 279, 46686–46691.
[83] Erkens, A., Schneider, K. and Müller, A. (1996) The NAD-linked soluble hydrogenase from *Alcaligenes eutrophus* H16: detection and characterization of EPR signals deriving from nickel and flavin. J. Biol. Inorg. Chem. 1, 99–110.
[84] Schneider, K., Cammack, R., Schlegel, H.G. and Hall, D.O. (1979) The iron-sulphur centres of soluble hydrogenase from *Alcaligenes eutrophus*. Biochim. Biophys. Acta 578, 445–461.
[85] Teixeira, M., Moura, I., Xavier, A.V., Moura, J.J., LeGall, J., DerVartanian, D.V., Peck, H.D. and Huynh, B.H. (1989) Redox intermediates of *Desulfovibrio gigas* [NiFe] hydrogenase generated under hydrogen. Mössbauer and EPR characterization of the metal centers. J. Biol. Chem. 264, 16435–16450.
[86] Rousset, M., Montet, Y., Guigliarelli, B., Forget, N., Asso, M., Bertrand, P., Fontecilla-Camps, J.C. and Hatchikian, E.C. (1998) [3Fe-4S] to [4Fe-4S] cluster conversion in *Desulfovibrio fructosovorans* [NiFe] hydrogenase by site-directed mutagenesis. Proc. Natl. Acad. Sci. USA 95, 11625–11630.
[87] Asso, M., Guigliarelli, B., Yagi, T. and Bertrand, P. (1992) EPR and redox properties of *Desulfovibrio vulgaris* Miyazaki hydrogenase: comparison with the NiFe enzyme from *Desulfovibrio gigas*. Biochim. Biophys. Acta 1122, 50–56.
[88] Horch, M., Lauterbach, L., Saggu, M., Hildebrandt, P., Lendzian, F., Bittl, R., Lenz, O. and Zebger, I. (2010) Probing the active site of an O_2-tolerant NAD^+-

reducing [NiFe]-hydrogenase from *Ralstonia eutropha* H16 by in situ EPR and FTIR spectroscopy. Angew. Chem. Int. Ed. 49, 8026–8029.
[89] Germer, F., Zebger, I., Saggu, M., Lendzian, F., Schulz, R. and Appel, J. (2009) Overexpression, isolation, spectroscopic characterization of the bidirectional [NiFe] hydrogenase from Synechocystis sp. PCC 6803. J. Biol. Chem. 284, 36462–36472.
[90] Lauterbach, L., Liu, J., Horch, M., Hummel, P., Schwarze, A., Haumann, M., Vincent, K.A., Lenz, O. and Zebger, I. (2011) The hydrogenase subcomplex of the NAD^+-reducing [NiFe] hydrogenase from *Ralstonia eutropha* - insights into catalysis and redox interconversions. Eur. J. Inorg. Chem. 2011, 1067–1079.
[91] McIntosh, C.L., Germer, F., Schulz, R., Appel, J. and Jones, A.K. (2011) The [NiFe]-hydrogenase of the cyanobacterium *Synechocystis* sp. PCC 6803 works bidirectionally with a bias to H_2 production. J. Am. Chem. Soc. 133, 11308–11319.
[92] Vincent, K.A., Parkin, A., Lenz, O., Albracht, S.P.J., Fontecilla-Camps, J.C., Cammack, R., Friedrich, B. and Armstrong, F.A. (2005) Electrochemical definitions of O_2 sensitivity and oxidative inactivation in hydrogenases. J. Am. Chem. Soc. 127, 18179–18189.
[93] Schneider, K., Cammack, R. and Schlegel, H.G. (1984) Content and localization of FMN, Fe-S clusters and nickel in the NAD-linked hydrogenase of *Nocardia opaca* 1b. Eur. J. Biochem. 142, 75–84.
[94] Zaborosch, C., Köstert, M., Bill, E., Schneider, K., Schlegel, H.G. and Trautweint, A.X. (1995) EPR and Mössbauer spectroscopic studies on the tetrameric, NAD-linked hydrogenase of *Nocardia opaca* 1b and its two dimers: 1. The βδ-dimer – a prototype of a simple hydrogenase. BioMetals 8, 149–162.
[95] Serebryakova, L.T., Medina, M., Zorin, N.A., Gogotov, I.N. and Cammack, R. (1996) Reversible hydrogenase of *Anabaena variabilis* ATCC 29413: catalytic properties and characterization of redox centres. FEBS Lett. 383, 79–82.
[96] van der Linden, E., Burgdorf, T., de Lacey, A., Buhrke, T., Scholte, M., Fernandez, V., Friedrich, B. and Albracht, S. (2006) An improved purification procedure for the soluble [NiFe]-hydrogenase of *Ralstonia eutropha*: new insights into its (in)stability and spectroscopic properties. J. Biol. Inorg. Chem. 11, 247–260.
[97] Silva, P.J., de Castro, B. and Hagen, W.R. (1999) On the prosthetic groups of the NiFe sulfhydrogenase from *Pyrococcus furiosus*: topology, structure, and temperature-dependent redox chemistry. J. Biol. Inorg. Chem. 4, 284–291.
[98] Grzeszik, C., Lübbers, M., Reh, M. and Schlegel, H.G. (1997) Genes encoding the NAD-reducing hydrogenase of *Rhodococcus opacus* MR11. Microbiology 143, 1271–1286.
[99] Albracht, S.P.J. and Hedderich, R. (2000) Learning from hydrogenases: location of a proton pump and of a second FMN in bovine NADH-ubiquinone oxidoreductase (Complex I). FEBS Lett. 485, 1–6.
[100] Hornhardt, S., Schneider, K. and Schlegel, H.G. (1986) Characterization of a native subunit of the NAD-linked hydrogenase isolated from a mutant of *Alcaligenes eutrophus* H16. Biochimie 68, 15–24.
[101] Tran-Betcke, A., Warnecke, U., Bocker, C., Zaborosch, C. and Friedrich, B. (1990) Cloning and nucleotide sequences of the genes for the subunits of NAD-reducing hydrogenase of *Alcaligenes eutrophus* H16. J. Bacteriol. 172, 2920–2929.
[102] Schlesier, M. and Friedrich, B. (1981) In vivo inactivation of soluble hydrogenase of *Alcaligenes eutrophus*. Arch. Microbiol. 129, 150–153.
[103] Schneider, K. and Schlegel, H.G. (1981) Production of superoxide radicals by soluble hydrogenase from *Alcaligenes eutrophus* H16. Biochem. J. 193, 99–107.
[104] Malki, S., Saimmaime, I., De Luca, G., Rousset, M., Dermoun, Z. and Belaich, J.P. (1995) Characterization of an operon encoding an NADP-reducing hydrogenase in *Desulfovibrio fructosovorans*. J. Bacteriol. 177, 2628–2636.
[105] Meyer, J. and Gagnon, J. (1991) Primary structure of hydrogenase from *Clostridium pasteurianum*. Biochemistry 30, 9697–9704.
[106] Reda, T., Barker, C.D. and Hirst, J. (2008) Reduction of the iron-sulfur clusters in mitochondrial NADH:ubiquinone oxidoreductase (Complex I) by EuII-DTPA, a very low potential reductant. Biochemistry 47, 8885–8893.
[107] Albracht, S.P.J., van der Linden, E. and Faber, B.W. (2003) Quantitative amino acid analysis of bovine NADH:ubiquinone oxidoreductase (Complex I) and related enzymes. Consequences for the number of prosthetic groups. Biochim. Biophys. Acta 1557, 41–49.
[108] Löscher, S., Burgdorf, T., Zebger, I., Hildebrandt, P., Dau, H., Friedrich, B. and Haumann, M. (2006) Bias from H_2 cleavage to production and coordination changes at the Ni-Fe active site in the NAD^+-reducing hydrogenase from *Ralstonia eutropha*. Biochemistry 45, 11658–11665.
[109] Roessler, M.M., King, M.S., Robinson, A.J., Armstrong, F.A., Harmer, J. and Hirst, J. (2010) Direct assignment of EPR spectra to structurally defined iron-sulfur clusters in Complex I by double electron-electron resonance. Proc. Natl. Acad. Sci. USA 107, 1930–1935.
[110] Schneider, K. and Schlegel, H.G. (1978) Identification and quantitative determination of the flavin component of soluble hydrogenase from. Biochem. Biophys. Res. Commun. 84, 564–571.
[111] Pedroni, P., Volpe, A.D., Galli, G., Mura, G.M., Pratesi, C. and Grandi, G. (1995) Characterization of the locus encoding the [Ni-Fe] sulfhydrogenase from the archaeon *Pyrococcus furiosus*: evidence for a relationship to bacterial sulfite reductases. Microbiology 141, 449–458.
[112] Berrisford, J.M. and Sazanov, L.A. (2009) Structural is for the mechanism of respiratory Complex I. J. Biol. Chem. 284, 29773–29783.
[113] Hornhardt, S., Schneider, K., Friedrich, B., Vogt, B. and Schlegel, H.G. (1990) Identification of distinct NAD-linked hydrogenase protein species in mutants and nickel-deficient wild-type cells of *Alcaligenes eutrophus* H16. Eur. J. Biochem. 189, 529–537.
[114] van der Linden, E., Faber, B.W., Bleijlevens, B., Burgdorf, T., Bernhard, M., Friedrich, B. and Albracht, S.P.J. (2004) Selective release and function of one of the two FMN groups in the cytoplasmic NAD^+-reducing [NiFe]-hydrogenase from *Ralstonia eutropha*. Eur. J. Biochem. 271, 801–808.
[115] Buhrke, T., Lenz, O., Krauss, N. and Friedrich, B. (2005) Oxygen tolerance of the H_2-sensing [NiFe] hydrogenase from *Ralstonia eutropha* H16 is based on limited access of oxygen to the active site. J. Biol. Chem. 280, 23791–23796.
[116] Goris, T., Wait, A.F., Saggu, M., Fritsch, J., Heidary, N., Stein, M., Zebger, I., Lendzian, F., Armstrong, F.A., Friedrich, B. and Lenz, O. (2011) A unique iron-sulfur cluster is crucial for oxygen tolerance of a [NiFe]-hydrogenase. Nat. Chem. Biol. 7, 310–318.
[117] Bagley, K.A., Duin, E.C., Roseboom, W., Albracht, S.P.J. and Woodruff, W.H. (1995) Infrared-detectable group senses changes in charge density on the nickel center in hydrogenase from *Chromatium vinosum*. Biochemistry 34, 5527–5535.
[118] Darensbourg, M.Y., Lyon, E.J. and Smee, J.J. (2000) The bio-organometallic chemistry of active site iron in hydrogenases. Coord. Chem. Rev. 206–207, 533–561.
[119] Burgdorf, T., Löscher, S., Liebisch, P., van der Linden, E., Galander, M., Lendzian, F., Meyer-Klaucke, W., Albracht, S.P.J., Friedrich, B., Dau, H. and Haumann, M. (2004) Structural and oxidation-state changes at its nonstandard Ni-Fe site during activation of the NAD-reducing hydrogenase from *Ralstonia eutropha* detected by X-ray absorption, EPR, and FTIR spectroscopy. J. Am. Chem. Soc. 127, 576–592.
[120] Gu, Z., Dong, J., Allan, C.B., Choudhury, S.B., Franco, R., Moura, J.J.G., Moura, I., LeGall, J., Przybyla, A.E., Roseboom, W., Albracht, S.P.J., Axley, M.J., Scott, R.A. and Maroney, M.J. (1996) Structure of the Ni sites in hydrogenases by X-ray absorption spectroscopy. Species variation and the effects of redox poise. J. Am. Chem. Soc. 118, 11155–11165.
[121] Müller, A., Henkel, G., Erkens, A., Schneider, K., Müller, A., Nolting, H.F. and Sole, V.A. (1997) NADH-induced changes of the nickel coordination within the active site of the soluble hydrogenase from *Alcaligenes eutrophus*: XAFS investigations on three states distinguishable by EPR spectroscopy. Angew. Chem. Int. Ed. Engl. 36, 1747–1750.
[122] Nakamoto, K. (2009) In *Infrared and Raman Spectra of Inorganic and Coordination Compounds - Applications in Coordination, Organometallic, and Bioinorganic Chemistry*, John Wiley and Sons, Inc., Hoboken, New Jersey. pp. 190–193.
[123] Cotton, F.A. and Wilkinson, G. (1988) In *Advanced Inorganic Chemistry*, John Wiley and Sons, Inc., New York. pp. 1299–1300.
[124] Johannssen, W., Gerberding, H., Rohde, M., Zaborosch, C. and Mayer, F. (1991) Structural aspects of the soluble NAD-dependent hydrogenase isolated from *Alcaligenes eutrophus* H16 and from *Nocardia opaca* 1b. Arch. Microbiol. 155, 303–308.
[125] Maroti, J., Farkas, A., Nagy, I.K., Maroti, G., Kondorosi, E., Rakhely, G. and Kovacs, K.L. (2010) A second soluble Hox-type NiFe enzyme completes the hydrogenase set in *Thiocapsa roseopersicina* BBS. Appl. Environ. Microbiol. 76, 5113–5123.